

## Transport of Energetic Particles by Microturbulence in Magnetized Plasmas

Wenlu Zhang (张文禄),<sup>1,2,\*</sup> Zhihong Lin (林志宏),<sup>1</sup> and Liu Chen (陈骝)<sup>1,3</sup>

<sup>1</sup>Department of Physics and Astronomy, University of California, Irvine, California 92697, USA

<sup>2</sup>CAS Key Laboratory of Basic Plasma Physics, University of Science and Technology of China, Hefei, Anhui 230026, China

<sup>3</sup>Institute for Fusion Theory and Simulation, Zhejiang University, Hangzhou, Zhejiang 310058, China

(Received 20 May 2008; published 27 August 2008)

Transport of energetic particles by the microturbulence in magnetized plasmas is studied in gyrokinetic simulations of the ion temperature gradient turbulence. The probability density function of the ion radial excursion is found to be very close to a Gaussian, indicating a diffusive transport process. The particle diffusivity can thus be calculated from a random walk model. The diffusivity is found to decrease drastically for high energy particles due to the averaging effects of the large gyroradius and orbit width, and the fast decorrelation of the energetic particles with the waves.

DOI: [10.1103/PhysRevLett.101.095001](https://doi.org/10.1103/PhysRevLett.101.095001)

PACS numbers: 52.25.Fi, 52.35.Ra, 52.55.Fa, 52.65.Tt

Energetic particles can be generated in magnetically confined plasmas by fusion reactions and auxiliary heating. They can be subjected to the diffusion by macroinstabilities [1], microturbulences [2], a stochastic magnetic field [3], and classical collisional and orbital effects [4]. The confinement of the energetic particles is a critical issue in the International Thermonuclear Experimental Reactor (ITER) [5], since the ignition relies on self-heating by the energetic fusion products. The diffusion of the energetic particles such as the cosmic rays by microscopic turbulence is also an important scientific issue in the space and astrophysical plasmas [6]. Earlier fusion experimental [4,7] and theoretical [8] studies indicated that energetic particles do not suffer a large transport due to the microturbulence excited by the pressure gradients of thermal particles. However, a recent fusion experiment [9] showed some evidence of the correlation between the excitation of the microturbulence and the redistribution of energetic ions produced by the neutral beam injection (NBI). Some recent theoretical [10] and computational [11] studies also suggested a significant transport level of the energetic particles driven by the microturbulence.

To resolve this discrepancy, here we study the diffusion of the energetic particles by the microscopic ion temperature gradient (ITG) [2] turbulence in large scale first-principles simulations of fusion plasmas using the global gyrokinetic toroidal code (GTC) [12]. The ion radial spread as a function of energy and pitch angle is measured in the steady-state ITG turbulence. The probability density function of the radial excursion is found to be very close to a Gaussian, indicating a diffusive transport from a random walk process. The radial diffusivity as a function of the energy and pitch angle can thus be calculated using the random walk model. We find that the diffusivity decreases drastically for high energy particles due to the averaging effects of the large gyroradius and banana width, and the fast decorrelation of the energetic particles with the ITG oscillations. By performing the integration in phase space,

we can calculate the diffusivity for any distribution function. The NBI ion diffusivity driven by the ITG turbulence is found to decrease rapidly for the born energy up to an order of magnitude of the plasma temperature and more gradually to a very low level for higher born energy. This result may explain the differences between the older experiments [4] with a higher born energy and the newer experiment [9] with a lower born energy (relative to the plasma temperature).

*Fully self-consistent ITG turbulence simulation.*— This study employed a well bench-marked, massively parallel full torus gyrokinetic toroidal code (GTC) and used representative parameters of tokamak *H*-mode core plasmas which have a peak temperature gradient of thermal ions at a radial position  $r = 0.5a$  with the following local parameters:  $R_0/L_T = 6.9$ ,  $R_0/L_n = 2.2$ ,  $q = 1.4$ ,  $\hat{s} \equiv (r/q)(dq/dr) = 0.78$ ,  $T_e/T_i = 1$ , and  $\epsilon \equiv a/R_0 = 0.36$ . Here  $R_0$  is the major radius,  $a$  is the minor radius,  $L_T$  and  $L_n$  are the temperature and density gradient scale lengths, respectively,  $T_i$  and  $T_e$  are the ion and electron temperature, and  $q = 0.854 + 2.184(r/a)^2$  is the safety factor. In the full torus nonlinear simulation of a  $a = 500\rho_i$  tokamak with  $\rho_i$  measured at  $r = 0.5a$ , we calculated 800 transit times of  $4 \times 10^8$  bulk marker particles (guiding centers), and interactions of these particles with self-consistent electrostatic potential represented on  $4 \times 10^7$  spatial grid points to address realistic reactor-grade plasma parameters covering disparate spatial and temporal scales. A more complete simulation model is described in Ref. [13]. The simulation starts with very small random fluctuations which grow exponentially due to the toroidal ITG instability as evident in the early part of the time history of the ion heat conductivity shown in the lower panel of Fig. 1. Zonal flows are then generated through modulational instability [14,15] and the ITG instabilities are saturated at the time of  $t = 250L_T/v_i$  through random shearing by the zonal flows [16]. Finally, the nonlinear coupling of ITG-zonal flows leads to a fully developed turbulence after

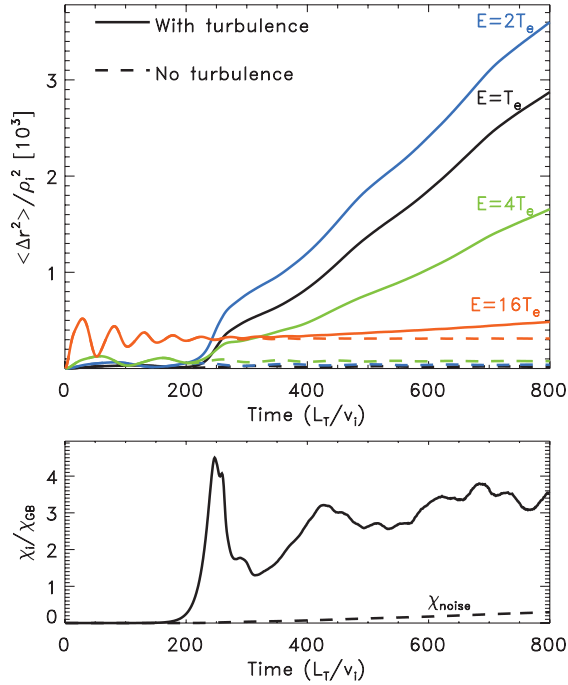


FIG. 1 (color). Lower panel: Time history of the thermal ion heat conductivity  $\chi_i$  driven by ITG turbulence (solid) or by particle noise (dashed). Upper panel: Time history of the radial excursion  $\langle \Delta r^2 \rangle$  for particle energy  $E/T_e = 1$  (black), 2 (blue), 4 (green), 16 (orange) when the ITG turbulence is present (solid) or absent (dashed).

$t = 400L_T/v_i$  with an ion heat conductivity of  $\chi_i = 3.1\chi_{GB}$  when averaging over  $t = [400, 800]L_T/v_i$ . The gyro-Bohm unit for the heat conductivity of the thermal ions are defined as  $\chi_{GB} = \rho^* \chi_B$ , where  $\rho^* = \rho_i/a$  and  $\chi_B = cT_e/(eB)$ . Here  $c$  and  $e$  are the speed of light and electric charge of electron. The fluctuations in the steady state are nearly isotropic in radial and poloidal directions [13] with the perpendicular spectrum peaks at  $k_{\perp}\rho_i = 0.15$ . GTC simulations of this ITG turbulence with similar parameters to study the size scaling [17] of the ITG transport and the turbulence spreading [13] that underlies the transition of the size scaling have previously been carried out with extensive numerical convergences. In particular, convergence with respect to the number of particles is carefully studied to ensure that the particle noise does not affect the physics being studied. We find that the noise-driven flux [18] is consistently smaller than the ITG-driven flux by at least an order of magnitude when using 10 particles per cell, as shown in the lower panel of Fig. 1.

*Statistics of ion radial diffusion.*—In order to study the transport of energetic particles by the ITG turbulence, we measure the radial diffusion of the ions, especially for the high energy tails of the distribution function. For this purpose, we calculate the radial excursion of several groups of ions in the phase space, specifically, a mesh of 17 grids in the energy  $E = mv^2/2$  (up to  $64T_e$ ) and 40 grids in the pitch angle  $\xi = v_{\parallel}/v$ , where  $v_{\parallel}$  is the local parallel velocity. For each velocity grid point, we initiate  $N =$

50 000 particles uniformly distributed in the radial domain of  $r/a = [0.45, 0.55]$  where the intensity of the turbulence is maximal. We calculate the mean-squared radial displacement of each group of particles  $\langle \Delta r^2 \rangle = N^{-1} \sum_{i=1}^N [r_i(t) - r_i(0)]^2$ , where  $r_i(0)$  and  $r_i(t)$  are the radial position of the  $i$ th particle at time  $t = 0$  and time  $t$ , respectively. The time history of the radial displacements for several energy groups (averaged over the pitch angle) are shown as the solid lines in the upper panel of Fig. 1. To isolate the effects of turbulence scattering, we also calculate the radial displacements of the same ions in another simulation where the ITG turbulence is suppressed. These displacements of the equilibrium orbits are plotted as dashed lines in the same figure. After a few bounce times  $\tau = 2\pi qR/(\sqrt{\epsilon}v)$ , the equilibrium displacements reach fixed amplitudes that are proportional to the energy as expected. Furthermore, the equilibrium displacements (dashed lines) are identical to the perturbed displacements (solid lines) for all energy groups before the turbulence grows to a high amplitude ( $t < 200L_T/v_i$ ). After the turbulence reach a steady state ( $t > 400L_T/v_i$ ), the difference between the equilibrium and perturbed displacements is small for high energy ions (e.g.,  $E = 16T_e$ ), indicating that the effect of the turbulence on the high energy orbits is small. On the other hand, for a lower energy (e.g.,  $E = 2T_e$ ), the perturbed displacement is much larger than the equilibrium displacement, indicating that the effect of the turbulence scattering dominates the radial displacement. An important feature in these results is that the net turbulent displacement (perturbed displacement subtracted by the equilibrium displacement) increases linearly with time for all energy groups in the steady-state ITG turbulence. This feature indicates that the radial excursion of the ions due to the turbulence scattering is a diffusive process.

The diffusive process is confirmed by the probability density function (PDF) of the radial displacement for each energy group. The PDF obtained at  $t = 800L_T/v_i$  is indeed very close to a Gaussian as shown in the upper panel of Fig. 2. Here, the skewness is  $S = \sqrt{N} \sum_{i=1}^N (x_i - \bar{x})^3 / (\sum_{i=1}^N (x_i - \bar{x})^2)^{3/2}$  and the kurtosis  $K = N \sum_{i=1}^N (x_i - \bar{x})^4 / (\sum_{i=1}^N (x_i - \bar{x})^2)^2 - 3$ . Consistent with the trend of the mean-squared displacements in Fig. 1, the standard deviation of the PDF in Fig. 2 decreases with increasing energy after it peaks at an energy of  $E = 2T_e$ . This peak energy is found to be consistent with the toroidal resonance condition for the ITG modes. That is, the drift resonance condition of  $\omega = \omega_d$  is satisfied at  $E = 2.1T_e$  when averaging over the pitch angle. Here the drift frequency is  $\omega_d = k_{\theta}v_d$ ,  $v_d = (v^2 + v_{\parallel}^2)/(R\Omega)$ , and the ITG frequency is  $\omega = k_{\theta}v_{ph}$ , where  $\Omega$  is the ion cyclotron frequency and  $k_{\theta} = nq/r$ . The linear phase velocity  $v_{ph}$  is measured in the simulation and is roughly a constant [13] for the modes of  $k_{\theta}\rho_i = [0, 0.3]$ , which have significant amplitudes in the nonlinear state.

The diffusive nature of the ITG turbulent transport is further supported by the fact that the radial profile of the

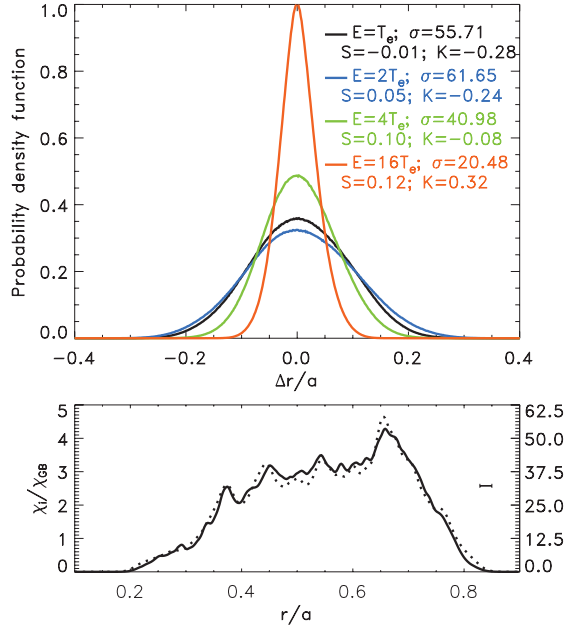


FIG. 2 (color). *Lower panel:* Radial profiles for thermal ion heat conductivity  $\chi_i$  and ITG intensity of fluctuating potential  $I = (\epsilon \delta \phi / \rho^* T_e)^2$ . *Upper panel:* Probability density functions of the radial excursion  $\Delta r/a$  for particle energy  $E/T_e = 1$  (black), 2 (blue), 4 (green), 16 (orange).  $\sigma$ ,  $S$ , and  $K$  are the standard deviation (in unit of  $\rho_i$ ), skewness, and kurtosis, respectively.

heat conductivity matches very well with the intensity profile as shown in the lower panel of Fig. 2; i.e., the transport is driven by the local fluctuation [13]. Furthermore, the PDF of the intensity of the fluctuating electrostatic potential, of the ion heat fluxes, and of the radial excursions all decay exponentially with no significant tails at large amplitudes. We conclude that the heat flux is carried by the radial diffusion of particles, and that large transport events, where heat pulses propagate ballistically, are apparently absent over this simulation time. Fundamentally, the stochastic wave-particle decorrelation [19] due to the overlaps of the phase-space islands gives rise to the diffusive transport process. That is, the wave does not trap or convect the particles, but only scatters the particle orbits.

*Transport of energetic particles.*—Since the radial excursion of the ions is diffusive, a phase-space-resolved diffusivity can be defined using the random walk model  $D(E, \xi) = \Delta \sigma^2 / (2\Delta t)$ , where  $\Delta \sigma^2$  is the change of the PDF standard deviation of the net radial displacement for each group of ions with energy  $E$  and pitch angle  $\xi$  during a time interval of  $\Delta t$  between  $t = 400L_T/v_i$  and  $t = 800L_T/v_i$  (when the turbulence is in a steady state). This radial diffusivity as a function of  $(E, \xi)$  is plotted in Fig. 3. The diffusivity is relatively smooth across the pitch angle  $\xi$  with no sharp resonance in the entire phase space. This is consistent with the diffusive process and the transport could therefore be described by a quasilinear theory [19]. As a consistency check, we calculate the diffusivity of the

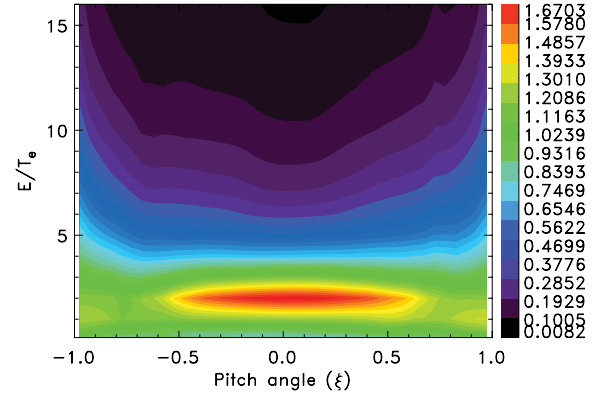


FIG. 3 (color). Diffusivity  $D/D_i$  as a function of particle energy  $E/T_e$  and pitch angle  $\xi$ .

thermal ions by averaging the diffusivity  $D$  over a Maxwellian distribution function with a temperature of  $T_e$ ,  $D_0 = \int DF_M d^3 \mathbf{v}$ . We find that this diffusivity  $D_0$  based on the random walk model is very close to an effective particle diffusivity  $D_i$  of thermal ions measured in the simulation,  $D_0 = 1.1D_i$ . Here  $D_i = 2\chi_i/3$  and  $\chi_i = 3.1\chi_{GB}$  calculated from the self-consistent heat flux using  $\chi_i = Q_i / (dT/dr)$ ,  $Q_i = \int \frac{1}{2} v^2 \delta v_r \delta f d^3 \mathbf{v}$  measured in the simulation, where  $v$  is particle velocity,  $\delta f$  is the perturbed distribution function, and  $\delta v_r$  is the radial component of gyrophase-averaged  $\mathbf{E} \times \mathbf{B}$  drift. Note that the particles used to measure the radial diffusion are part of the plasma with both drag and scattering effects. However, the scattering effect dominates the radial diffusion (similar to test particles) because of the constraints of the quasineutrality and adiabatic electrons.

The diffusivity shown in Fig. 3 peaks at the resonant energy of  $E = 2T_e$  and decreases drastically for higher energy particles. This is due to the averaging effects of the large gyroradius and orbital width, and the fast decorrelation of the energetic particles with the waves for the high energy particles. To understand the physical mechanisms of the reduction of the diffusivity for energetic particle, we examine the scaling of the diffusivity with respect to the particle energy. Taking a cut of  $\xi = 0$  in Fig. 3, we find that the diffusivity  $D \propto 1/E^2$  for trapped energetic particles with  $E > 3T_e$ . This scaling can be understood from the quasilinear theory of the diffusivity for trapped particles in the high energy limit,

$$D \propto \sum_n \frac{c^2 |k_r k_\theta \phi_n|^2}{B^2} J_0^2(k_\perp \rho_E) J_0^2(k_\perp \rho_b) \delta(\omega - \omega_d + p\omega_b).$$

Here the first Bessel function comes from the gyroaveraging and the second from the averaging over banana orbits,  $\omega_b = \sqrt{\epsilon} v_E / (2\pi q R)$  is the bounce frequency,  $\epsilon = r/R$  is the inverse aspect ratio,  $\rho_b$  is the banana width,  $\rho_E$  and  $v_E$  are the gyroradius and velocity of energetic particles, respectively,  $k_r$  and  $k_\theta$  are the wave number in the  $r$  and  $\theta$  direction,  $B$  is the magnetic field,  $\phi_n$  is the electrostatic potential, and  $p$  is the harmonics number. These two

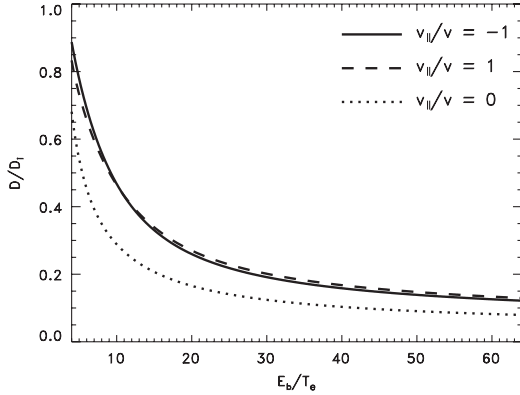


FIG. 4. Diffusivity for a slowing-down distribution as a function of the NBI beam ion born energy ( $E_b/T_e$ ) for passing (solid and dash) and trapped (dotted) particles.

averages give rise to a dependence of  $D$  on  $1/E$  when taking a large argument expansion of the Bessel function. Regarding the resonance condition, since  $\omega_d, \omega_b \gg \omega$  for energetic particles, we need  $p > 0$ . Therefore the resonance condition becomes  $\omega_d = p\omega_b$ , or equivalently,  $n\omega_{\text{pre}} = p\omega_b$ , where  $\omega_{\text{pre}} = qE/(mRr\Omega)$  is the precession frequency. This is the so-called drift-bounce resonance [20] underlying the ripple loss process, which gives rise to another dependence of  $D$  on  $1/E$  when integrating over  $n$  since  $\omega_{\text{pre}}$  is proportional to  $E$ . Hence, for energetic trapped particles, the diffusivity  $D \propto 1/E^2$  accounting both the orbit averaging and the decorrelation process. For passing particles, the resonance condition of  $\omega = k_{\parallel}v_{\parallel}$  and the orbital averaging will each give rise to a  $E^{-1/2}$  dependence of  $D$ , so we expect that a diffusivity  $D \propto 1/E$  for energetic passing particle. Indeed, when taking a cut of Fig. 3 at  $\xi = 1$  and  $-1$ , we find that the diffusivity  $D$  depends roughly on  $1/E$  for  $E > 20T_e$ . These different scalings result in a larger diffusivity for the energetic passing particles than the energetic trapped particles as shown in Fig. 3.

The measured diffusivity in phase space as shown in Fig. 3 provides all information for calculating the diffusivity for arbitrary distribution function of energetic ions by taking integration over the energy and pitch angle. Of particular interest is the diffusivity for the NBI ions since most existing fusion experiments use the NBI heating. A steady-state slowing-down distribution function [21] is commonly used to describe the energetic NBI ions in a background plasma consisting of thermal ions and electrons. By solving the Fokker-Planck equation including a source term in both velocity and pitch angle,  $S = \frac{S_0}{2\pi\sqrt{2E}} \delta(E - E_b) \delta(\xi - \xi_b)$ , the corresponding slowing-down distribution is formulated in term of Legendre polynomials,  $f_b(E, \xi) = \frac{S_0\tau_s H(E_b - E)}{E_c^{3/2} + E^{3/2}} \sum_{l=0}^{\infty} C_l(E) P_l(\xi_b) P_l(\xi)$ , where  $H(E_b - E)$  is the Heaviside step function,  $\tau_s$  is the Spitzer slowing-down time,  $E_c$  is the critical energy,  $E_b$ ,  $\xi_b$ , and  $S_0$  are the born speed, pitch angle, and source intensity of ener-

getic particle. We now use this slowing-down distribution to calculate the diffusivity for energetic NBI ions  $D(E_b, \xi_b) = \overline{f(E, \xi) D(E, \xi) / f(E, \xi)}$ , where  $d\mathbf{v}^3 = 2\pi v^2 dv d\xi = 2\pi\sqrt{2E} dE d\xi$ ,  $\overline{f(E, \xi)} = \int_{E_{\text{min}}}^{E_b} \sqrt{2E} dE \times \int_{-1}^1 d\xi f(E, \xi)$  is the phase-space integration, and  $E_{\text{min}} = 4T_e$  is a heuristic cutoff energy separating thermal and energetic particles in our calculation. The diffusivity for the energetic particles as a function of the born energy  $E_b$  is calculated as shown in Fig. 4. It shows that the NBI beam diffusivity is significant for the low born energy with  $E_b < 10T_e$ , and decays very fast when  $E_b < 20T_e$ . For higher born energy, it gradually approaches to a low level of 10% to 15% of the diffusivity of the thermal particles. These results may explain the differences between the older experiments with a higher born energy of energetic particles and the newer experiment with a lower born energy of energetic particles.

The authors acknowledge the computational contributions by Y. Nishimura and V. Decyk. We would like to thank P. H. Diamond, W. Heidbrink, I. Holod, R. E. Waltz and Y. Xiao for useful discussions. This work was supported by the U. S. Department of Energy (DOE) SciDAC GSEP, and GPS centers, and by DOE and NSF grants. Simulations used supercomputers at NERSC and ORNL.

\*wenluz@uci.edu

- [1] C. Z. Cheng, L. Chen, and M. S. Chance, *Ann. Phys. (N.Y.)* **161**, 21 (1985).
- [2] W. Horton, *Rev. Mod. Phys.* **71**, 735 (1999).
- [3] A. B. Rechester and M. N. Rosenbluth, *Phys. Rev. Lett.* **40**, 38 (1978).
- [4] W. W. Heidbrink and G. J. Sadler, *Nucl. Fusion* **34**, 535 (1994).
- [5] <http://www.iter.org>.
- [6] J. Giacalone and J. R. Jokipii, *Astrophys. J.* **520**, 204 (1999).
- [7] S. J. Zweben *et al.*, *Nucl. Fusion* **40**, 91 (2000).
- [8] G. Manfredi and R. O. Dendy, *Phys. Rev. Lett.* **76**, 4360 (1996).
- [9] S. Gunter *et al.*, *Nucl. Fusion* **47**, 920 (2007).
- [10] M. Vlad and F. Spineanu, *Plasma Phys. Controlled Fusion* **47**, 281 (2005).
- [11] C. Estrada-Mila, J. Candy, and R. E. Waltz, *Phys. Plasmas* **13**, 112303 (2006).
- [12] Z. Lin *et al.*, *Science* **281**, 1835 (1998).
- [13] Z. Lin and T. S. Hahm, *Phys. Plasmas* **11**, 1099 (2004).
- [14] P. Diamond *et al.*, in *Proc. 17th IAEA Fusion Energy Conf. on Controlled Fusion and Plasma Physics* (Yokohama, Japan, 1998).
- [15] L. Chen, Z. H. Lin, and R. White, *Phys. Plasmas* **7**, 3129 (2000).
- [16] T. S. Hahm *et al.*, *Phys. Plasmas* **6**, 922 (1999).
- [17] Z. Lin *et al.*, *Phys. Rev. Lett.* **88**, 195004 (2002).
- [18] I. Holod and Z. Lin, *Phys. Plasmas* **14**, 032306 (2007).
- [19] Z. Lin *et al.*, *Phys. Rev. Lett.* **99**, 265003 (2007).
- [20] L. Chen, *J. Geophys. Res., [Space Phys.]* **104**, 2421 (1999).
- [21] J. D. Gaffey, *J. Plasma Phys.* **16**, 149 (1976).